

High-Field Scanning Probe Lithography in Hexadecane: Transitioning from Field Induced Oxidation to Solvent Decomposition through Surface Modification**

By Itai Suez, Marco Rolandi, Scott A. Backer, Andreas Scholl, Andrew Doran, David Okawa, Alex Zettl, and Jean M. J. Fréchet*

In the recent past, a variety of scanning-probe techniques^[1–3] have been employed to generate nanometer-size structures on semiconducting,^[4–10] metallic,^[11,12] and organic surfaces.^[13–19] In general, these methods utilize the proximity of the scanning probe to generate an intense electric field (ca. 10^9 V m⁻¹) by applying a relatively low bias of the order of a few volts. The oxidation of silicon in air using surface adsorbed water as the medium between tip and substrate has been studied most extensively.^[4–10] Field-induced techniques have been employed to pattern larger areas in parallel through the use of a stamp coated with conducting material.^[20–22] The ultimate lateral resolution of field-induced lithography is directly related to the dimensions of the protruding features of the stamp or the sharpness of the scanning probe.

Recently, there have been ongoing efforts to replace the water in the tip/substrate gap with organic solvents in order to explore novel field-induced chemical reactions.^[23–29] For example, the deposition of etch resistant features was previously demonstrated in our laboratories^[24] using common solvents such as toluene, n-octane, ethyl alcohol, and dioxane as the medium between the sample and the tip of an atomic force microscope (AFM) operated in fluid. Similarly, recent work was performed by Garcia and co-workers^[23,26] using an ethyl

alcohol meniscus in the tip/substrate gap. Most recently, the same group has achieved <5 nm resolution using a solvent meniscus condensed from octane vapour.^[27] Of particular relevance to our work, are the findings reported by Hersam and co-workers^[28,29] for contact mode patterning in hexadecane on H:Si(111). Both the growth kinetics and the chemical behavior of the deposited features were consistent with field induced oxidation (FIO) of silicon. The authors conclude that oxidation of the silicon surface occurs in the meniscus formed between the probe and the surface by the water dissolved in the fluid, with minimal effects on the reaction from the surrounding solvent. It is important to note that the water content in hexadecane is reported to be three-fold higher than that found in n-octane at same pressure and humidity.^[30]

In the present work, the role of surface hydrophobicity in the high field scanning probe nanolithography in hexadecane is investigated. A schematic representation of the setup employed is shown in Figure 1a. In this setup, both the probe of the atomic force microscope and the sample are immersed in the solvent to carry out the patterning and the initial imaging of the nanostructures. For patterning, a potential difference is applied between the probe and the sample (positive on the sample) while the tip is translated across the desired location kept in close proximity to the surface. The results obtained after patterning both a hydrophilic silicon oxide surface (contact angle ca. 0°) and hydrophobic TMS terminated surface (contact angle 90°) were investigated using the process flow shown in Figure 1b. The hydrophobic surface was obtained via passivation of the surface of the silicon wafer with hexamethyldisilazane (HMDS).

When high field lithography in hexadecane was performed on the hydrophilic surface, feature growth rates consistent with FIO of silicon were observed.^[4,28,29] In Figure 2a, the 1.5 nm tall features that are observed were fabricated at a scan rate of 1 $\mu\text{m s}^{-1}$ with a 12 V bias applied on the sample. In contrast, when the HMDS surface-modified substrate was used (Fig. 2b), the growth rate was significantly faster and found to be consistent with what had previously been reported for the high field decomposition of n-octane, toluene, ethyl alcohol, and dioxane under the same exposure conditions.^[24–27] In Figure 2b, (2.2 ± 0.2) nm tall lines were fabricated on the HMDS-protected silicon surface at a scan rate of 15 $\mu\text{m s}^{-1}$ with a 12 V bias applied on the sample. A comparison of the relative scan speeds and heights of the features

[*] Prof. J. M. J. Fréchet, Dr. I. Suez, Dr. M. Rolandi, Dr. S. A. Backer, D. Okawa
College of Chemistry, University of California
Berkeley, CA 94720 (USA)
E-mail: frechet@berkeley.edu

Prof. J. M. J. Fréchet, Dr. M. Rolandi, Prof. A. Zettl
Materials Sciences Division, Lawrence Berkeley National Laboratory
Berkeley, CA 94720 (USA)

Dr. A. Scholl, Dr. A. Doran
Advanced Light Source, Lawrence Berkeley National Laboratory
Berkeley, CA 94720 (USA)

Prof. A. Zettl
Department of Physics, University of California
Berkeley, CA 94720 (USA)

[**] Financial support of this research by NSF (SINAM and EEC-0425914), SRC-DARPA, and the Director, Office of Basic Energy Science, Office of Energy Research and Materials Sciences Division of the U.S. Department of Energy under Contract No.'s DE-AC02-05CH11231 and DE-AC03-76SF0098 is acknowledged with thanks. M.R. thanks INTEL for postdoctoral funding through the Materials Sciences Division, LBNL. The authors also thank Professor Calvin F. Quate for many helpful and stimulating discussions.

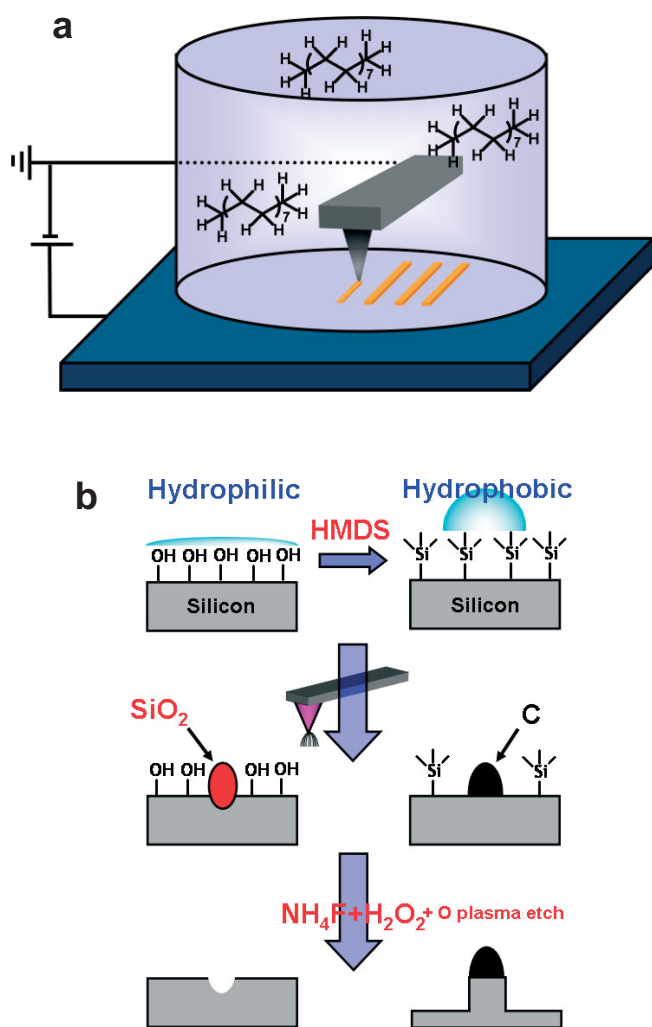


Figure 1. a) Representation of the set up for high-field scanning probe lithography in hexadecane. b) Schematic of the two patterning routes depending on surface hydrophilicity.

leads to an estimated 20-fold increase in vertical growth rate when changing from the hydrophilic surface to a hydrophobic surface.

Immersion of the patterns made on the hydrophilic surface into a bath containing a mild ammonium fluoride based etchant (10:3:100/ $\text{NH}_4\text{F}:\text{H}_2\text{O}_2:\text{H}_2\text{O}$) leads to the formation of shallow trenches as can be seen in Figure 2c and e. This again confirms the suggestion that the original features were primarily composed of silicon oxide, since silicon oxide is readily removed by fluorinated etchants.^[31] In contrast, the features made on the HMDS-passivated surface displayed a completely different behavior upon immersion in the same wet etch (Fig. 2d and f) as etching did not produce trenches but rather tall posts ca. 10 nm in height as shown in Figure 2f.^[32]

In order to better characterize the patterns made on the hydrophobic HMDS surface, high-resolution photoemission electron microscopy (PEEM) was performed on microscopic patches of material created as described above but on a larger

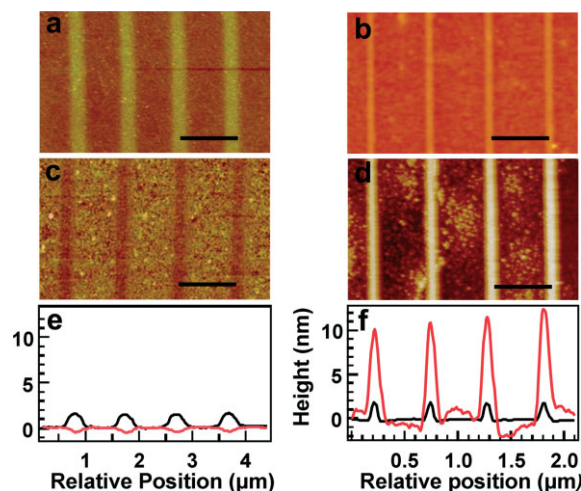


Figure 2. Atomic force microscope images and cross section of the different patterning steps. a) and b) AFM images of areas patterned using high field lithography in hexadecane a) SiO_2 lines patterned on the hydrophilic surface at $+12\text{ V } 1\ \mu\text{m s}^{-1}$ rate b) carbonaceous lines deposited on the hydrophobic surface at $+12\text{ V } 10\ \mu\text{m s}^{-1}$ rate, scale bars are $1\ \mu\text{m}$ and $0.5\ \mu\text{m}$, respectively. c) and d) same areas after etch transfer in a solution containing $\text{NH}_4\text{F} + \text{H}_2\text{O}_2$ note the tone reversal depending on the material deposited. e) and f) average of the cross sections of the patterned areas, black represents before and red represents after etch transfer.

area enabling application of the PEEM characterization technique (Fig. 3a).

The larger features were then investigated for both carbon content and type of bonding by performing electron yield experiments at energies below and above the carbon edge. The results obtained in these analytical explorations are shown in Figure 3b and c. Figure 3b is an image of the carbon signal on the sample after background subtraction to correct for any geometric effects. As can readily be observed, the areas with the highest carbon content (bright in the image) closely match the two patches on the AFM image of Figure 3a. Spectral information is presented in Figure 3c. The colored spectra correspond to the data taken from the PEEM after subtraction of the background signal of the detector and pre-edge normalization to compensate for different emission of the areas written with the AFM and the variation of the X-ray illumination across the image. The very strong dip in all the spectra corresponds to carbon contamination of the beamline optical components (e.g. gratings). Although there are only small differences in features of the local spectra, carbon content information was obtained by normalizing the spectra taken on the patches with the spectra in the background serving as an I_0 correction. It is important to note that the carbon contamination of this sample is rather high due to the presence of the organic monolayer on the surface.

The black line on the plot shows three distinct peaks, two sharp and one rather broad. By comparing these peaks with spectra taken on aromatic molecules on the same instrument^[33] we assigned the two first peaks to the transition of a photoelectron from the K shell of carbon to the first and the

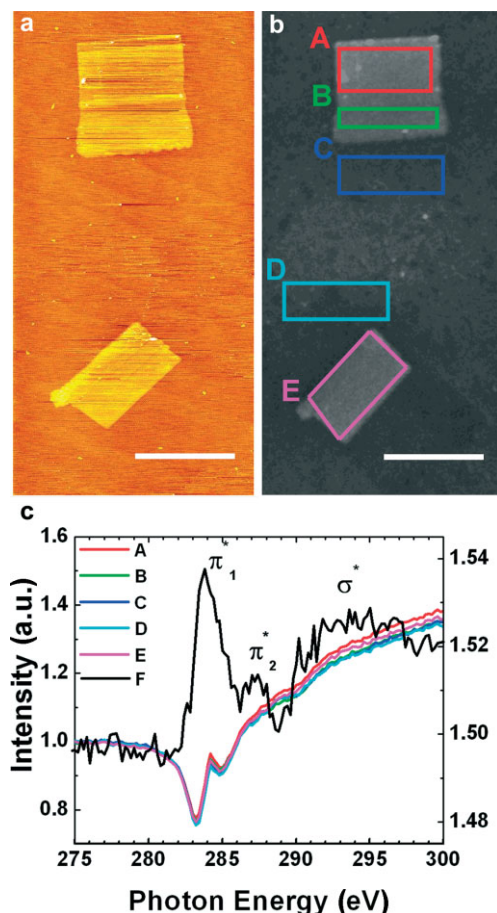


Figure 3. PEEM analysis of microscopic patterns. a) AFM image of two microscopic carbonaceous patterns deposited on the hydrophobic functionalized silicon surface, scale bar 10 μm . b) Carbon signal PEEM image taken at 290 eV corrected for background by subtracting an image taken at 270 eV of the same patterns. c) PEEM spectra acquired in the depicted area. Spectra a-f are normalized data colour coded and acquired in the boxes shown in image b), the dip is due to carbon contamination present on the beamline optics. Spectrum f is the result of subtracting the sum of the spectra taken in the background from the sum of the spectra taken on the patches after renormalization of the spectra for intensity correction.

second unoccupied π^* state of C=C double bond. These peaks are a clear signature for a high content of sp^2 hybridized carbon atoms in the patches. Furthermore, the broader peak can be identified with the transitions ending the excited σ molecular states corresponding to a smaller but still significant presence of sp^3 hybridized carbon atoms. This analysis confirms the carbonaceous content of the patches and gives some insights on the bonding network formed by tip exposure. The etch resistance of the material formed by tip exposure also resembles that achieved with materials having at least some aromatic or graphitic character. The transition of sp^3 hybridized carbon to aromatic compounds has previously been reported in organic monolayers exposed with low energy electrons (50 eV),^[34] thus, it is not unreasonable to imagine the solvent molecules incurring a similar transformation.

In summary, we have demonstrated that two possible chemical pathways exist for tapping mode high field lithography in simple materials such as hexadecane. On a hydrophilic surface, the water dissolved in the solvent forms a meniscus between the tip and the sample due to capillary condensation and displaces the solvent from the active region, this results in local field induced oxidation of the silicon substrate. This is consistent with previous reports of high-field lithography in hexadecane on H:Si(111), where patterning in contact mode affords a stable water meniscus even on a relatively hydrophobic surface (contact angle 79°).^[28,29] Alternatively, when patterning in tapping mode on the hydrophobic HMDS terminated surface, water cannot form a stable meniscus and the solvent present in the active region bears the brunt of the high energy modification process. Under such high field conditions, the solvent readily decomposes, depositing etch resistant features rich in sp^2 hybridized carbon. This study clarifies the modes of tip-induced nanoscale patterning that are available using simple solvents as “resists”. It is particularly noteworthy that a simple change in reaction conditions enables the tuning of the imaging tone from positive to negative or vice-versa.

Experimental

Si (100) substrates (Addising Engineering, p-type, boron-doped, resistivity 0.02–0.03 Ωcm^{-1}) were cleaned in a HF solution and a thin oxide layer ca. 1–2 nm was grown in an oxygen plasma as previously described [24]. Anhydrous hexadecane (0.0008% water, Sigma–Aldrich) was equilibrated in atmosphere prior to use. Patterning experiments were performed using a Digital Instruments Multimode atomic force microscope equipped with a fluid cell operated in tapping™ mode. Silicon cantilevers (force constant 2 N m^{-1} and resonant frequency ca. 75 kHz) coated with a conducting layer of Ti/Pt (VeecoProbes) were employed. Patterning was achieved in hexadecane by applying a positive bias (7–12 V) to the sample while translating the grounded tip across the desired locations on the surface. During this process, the tip sample separation was reduced until the amplitude of vibration of the tip reached 20% of the imaging set-point. The hydrophilic pristine surfaces were used immediately after oxidation with a water contact angle of ca. 0°. The hydrophobic surfaces were prepared by placing the freshly oxidized wafers into an enclosed container with a small pool of HMDS for several minutes. This resulted in a well packed and clean monolayer with a water contact angle of 90° \pm 2°. The spectromicroscopic characterization of the deposited material was performed at the microscopy branch (PEEM-2) of the beamline 7.3.1.1 at the Advanced Light Source at the Lawrence Berkeley National Laboratory in Berkeley, CA. The photon energy range of this branch is 250 eV to 1300 eV with a spectral resolving power between 1200 and 1800. The X-ray photoelectron microscope (PEEM) is operated in total electron yield (TEY) with a maximum spatial resolution of ca. 50 nm for elemental contrast imaging. Stacks of successive near edge X-ray absorption fine structure (NEXAFS) images over the photon energies containing the relevant C- edge were acquired in the grazing incident geometry. All the raw spectra were normalized to unity from 5 to 10 eV before the edge jump to compensate for geometric effects, work function and conductivity differences that foreshadow the chemical signal in the TEY mode.

Received: March 23, 2007

Revised: May 9, 2007

- [1] C. F. Quate, *Surf. Sci.* **1997**, *386*, 259.
- [2] J. Loos, *Adv. Mater.* **2005**, *17*, 1821.
- [3] R. Garcia, R. V. Martinez, J. Martinez, *Chem. Soc. Rev.* **2006**, *35*, 29.
- [4] P. Avouris, T. Hertel, R. Martel, *Appl. Phys. Lett.* **1997**, *71*, 285.
- [5] E. Snow, P. Campbell, *Appl. Phys. Lett.* **1994**, *64*, 1932.
- [6] J. A. Dagata, J. Schneir, H. H. Harary, C. J. Evans, M. T. Postek, J. Bennett, *Appl. Phys. Lett.* **1990**, *56*, 2001.
- [7] J. A. Dagata, T. Inoue, J. Itoh, K. Matsumoto, H. Yokoyama, *J. Appl. Phys.* **1998**, *84*, 6891.
- [8] E. Dubois, J. L. Bubendorff, *J. Appl. Phys.* **2000**, *87*, 8148.
- [9] R. Garcia, M. Calleja, F. Pérez-Murano, *Appl. Phys. Lett.* **1998**, *72*, 2295.
- [10] E. Stiévenard, P. A. Fontaine, E. Dubois, *Appl. Phys. Lett.* **1997**, *70*, 3272.
- [11] H. Sugimura, T. Uchida, N. Kitamura, H. Masuhara, *J. Phys. Chem.* **1994**, *98*, 4352.
- [12] M. Rolandi, C. F. Quate, H. Dai, *Adv. Mater.* **2002**, *14*, 191.
- [13] M. Rolandi, I. Suez, H. Dai, J. M. J. Fréchet, *Nano Lett.* **2004**, *4*, 889.
- [14] R. M. Penner, M. J. Heben, N. S. Lewis, C. F. Quate, *Appl. Phys. Lett.* **1991**, *58*, 1389.
- [15] D. C. Tully, K. Wilder, J. M. J. Fréchet, A. Trimble, C. F. Quate, *Adv. Mater.* **1999**, *11*, 314.
- [16] K. Wilder, C. F. Quate, D. Adderton, R. Bernstein, V. Eilings, *Appl. Phys. Lett.* **1998**, *73*, 2527.
- [17] G. Y. Liu, Y. L. Qian, *Acc. Chem. Res.* **2000**, *33*, 457.
- [18] M. Lercel, G. Redinbo, H. G. Craighead, C. W. Sheen, D. L. Allara, *Appl. Phys. Lett.* **1994**, *65*, 974.
- [19] X. N. Xie, M. Deng, H. Xu, S. W. Yang, D. C. Qi, X. Y. Gao, H. J. Chung, C. H. Sow, V. B. C. Tan, A. T. S. Wee, *J. Am. Chem. Soc.* **2006**, *128*, 2738.
- [20] M. Cavallini, P. Mei, F. Biscarini, R. Garcia, *Appl. Phys. Lett.* **2003**, *83*, 5286.
- [21] S. Hoepfener, R. Maoz, J. Sagiv, *Nano Lett.* **2003**, *3*, 761.
- [22] N. Farkas, J. R. Comer, G. Zhang, E. A. Evans, R. D. Ramsier, S. Wight, J. A. Dagata, *Appl. Phys. Lett.* **2004**, *85*, 5691.
- [23] M. Tello, R. Garcia, *Appl. Phys. Lett.* **2003**, *83*, 2339.
- [24] I. Suez, S. A. Backer, J. M. J. Fréchet, *Nano Lett.* **2005**, *5*, 321.
- [25] R. V. Martinez, R. Garcia, *Nano Lett.* **2005**, *5*, 1161.
- [26] M. Tello, R. Garcia, J. A. Martín-Gago, N. F. Martínez, M. S. Martín-González, L. Aballe, A. Baranov, L. Gregoratti, *Adv. Mater.* **2005**, *17*, 1480.
- [27] R. V. Martinez, N. S. Losilla, J. Martinez, Y. Huttel, R. Garcia, *Nano Lett.* **2007**, published online, March 13; DOI 10.1021/nl070328r.
- [28] C. R. Kinser, M. J. Schmitz, M. C. Hersam, *Nano Lett.* **2005**, *5*, 91.
- [29] C. R. Kinser, M. J. Schmitz, M. C. Hersam, *Adv. Mater.* **2006**, *18*, 1377.
- [30] C. Black, C. G. Joris, H. S. Taylor, *J. Chem. Phys.* **1948**, *16*, 537.
- [31] L. F. Thompson, C. G. Willson, M. J. Bowden, *Introduction to Microlithography*, 2nd ed., ACS, Washington, DC **1994**.
- [32] For this surface, prior to the wet etch, a low power oxidation in an RF plasma was implemented for 10 s. for removal of the surrounding organic monolayer. This plasma etch probably reduced the etch resistance of the patterns and cannot be responsible for the tone reversal effect.
- [33] M. Zharnikov, A. Shaporenko, A. Paul, A. Götzhäuser, A. Scholl, *J. Phys. Chem. B* **2005**, *109*, 5168.
- [34] M. Zharnikov, W. Geyer, A. Götzhäuser, S. Frey, M. Grunze, *Phys. Chem. Chem. Phys.* **1999**, *1*, 3163.